



LUND UNIVERSITY

Effects of dielectrics and internal resonances on modal analysis of terminal chassis

Miers, Zachary T.; Lau, Buon Kiong

Published in:

2016 10th European Conference on Antennas and Propagation, EuCAP 2016

DOI:

[10.1109/EuCAP.2016.7481130](https://doi.org/10.1109/EuCAP.2016.7481130)

2016

Document Version:

Peer reviewed version (aka post-print)

[Link to publication](#)

Citation for published version (APA):

Miers, Z. T., & Lau, B. K. (2016). Effects of dielectrics and internal resonances on modal analysis of terminal chassis. In *2016 10th European Conference on Antennas and Propagation, EuCAP 2016* Article 7481130 IEEE - Institute of Electrical and Electronics Engineers Inc.. <https://doi.org/10.1109/EuCAP.2016.7481130>

Total number of authors:

2

General rights

Unless other specific re-use rights are stated the following general rights apply:

Copyright and moral rights for the publications made accessible in the public portal are retained by the authors and/or other copyright owners and it is a condition of accessing publications that users recognise and abide by the legal requirements associated with these rights.

- Users may download and print one copy of any publication from the public portal for the purpose of private study or research.
- You may not further distribute the material or use it for any profit-making activity or commercial gain
- You may freely distribute the URL identifying the publication in the public portal

Read more about Creative commons licenses: <https://creativecommons.org/licenses/>

Take down policy

If you believe that this document breaches copyright please contact us providing details, and we will remove access to the work immediately and investigate your claim.

LUND UNIVERSITY

PO Box 117
221 00 Lund
+46 46-222 00 00

Effects of Dielectrics and Internal Resonances on Modal Analysis of Terminal Chassis

Zachary T. Miers, Buon Kiong Lau

Department of Electrical and Information Technology, Lund University, Lund, Sweden

Abstract—The symmetric PMCHWT method of moments (MoM) impedance matrix allows for the characteristic modes (CMs) of a structure containing dielectric to be found. Recently, this impedance matrix was proven to provide non-real solutions which can be attributed to the MoM internal resonance problem. These internal resonances can be removed through different CM post-processing techniques. However, these studies focus on dielectric structures, whereas the majority of antennas utilize electric conductors as the radiators. As such, dielectrics are often neglected to simplify the CM analysis and hence the problem of internal resonance is overlooked. This work explores the extent of the internal resonance problem in mixed conductor-dielectric structures. The results reveal that the problem is severe even when the structures only contain small amounts of dielectric materials. Moreover, the significant impact of dielectrics on CMs reveals that dielectrics should be included in CM analysis to ensure high accuracy.

Index Terms—Theory of Characteristic Modes, terminal antennas, method of moments, dielectric material.

I. INTRODUCTION

Shortly after the initial development of the Theory of Characteristic Modes (TCM) in [1], Harrington introduced a method for extracting the characteristic modes (CMs) of dielectric and magnetic bodies using a method of moments (MoM) volume integral equation (VIE) formulation [2]. This specific formulation produces a symmetric impedance matrix which can be used to solve for the CMs of an object. However, VIE formulations are computationally complex, and even electrically compact objects are difficult to solve using this method [3], [4].

As a computationally efficient alternative, a symmetric form of the MoM surface integral equation (SIE) was formulated in [5], along with a proof that this SIE formulation can be used to solve for the modal currents of any dielectric or magnetic body. However, it was shown in [4] and later proven in [6] that these modal currents are not equivalent to the characteristic currents of the object. The modal solution to the symmetric SIE impedance matrix provides an orthogonal set of both internal (non-real) and external (real) currents; these internal modes are related to the classical MoM internal resonance problem [3]. The set of currents which include the internal resonances does not provide a unique set of orthogonal far-fields, and furthermore the internal resonances cannot be excited and do not radiate far-field energy. Therefore, these internal currents do not satisfy the basic properties of CMs [1].

However, by applying any of the post-processing methods described in [4] and [6], the internal resonances can be

removed, with the remaining external (real) modes being equal to the complete set of CMs for the structure. Nevertheless, despite the recent progress in removing internal resonances from SIE solutions [4], [6], recent work has only focused on dielectric resonators, which are pure dielectric structures. The extent of the internal resonance problem has not been studied for other structures, such as a conventional terminal chassis which does not rely on dielectrics as the main radiators when used for antenna design. Moreover, the impact of dielectrics on the CMs of such structures is largely unknown.

In this article, a terminal chassis containing a small amount of dielectric material is analyzed using CMs. As will be shown, it is important to include the dielectric material in CM simulations, as the extracted CMs should match as closely as possible to the actual CMs of the real-world device. As the terminal chassis contains both conducting and dielectric materials, the symmetric form of the mixed material Poggio-Miller-Chan-Harrington-Wu-Tsai (PMCHWT) SIE MoM impedance matrix was used to solve for the structure's CMs. The results demonstrate that even when small amounts of dielectrics are used in terminal structures, the internal resonances cannot be ignored. Furthermore, this paper compares the resonant frequencies of the structure's CMs against those of excited antennas designed to utilize the corresponding CMs, with the latter obtained from Finite Element Method (FEM) simulations in CST.

II. MIXED MATERIAL ANALYSIS

Solving for the CMs of any object composed of multiple kinds of material is not identical to solving for the CMs of objects composed of a single kind of material. Papers [5] and [6] show that all existing MoM SIE implementations form an asymmetric impedance matrix, and this type of matrix does not guarantee proper diagonalization of the currents when using a suitably weighted eigenvalue equation. Therefore, a method of forcing a specific SIE solution into symmetry was proposed in [5]. The SIE equation set that was utilized is the PMCHWT surface integral equation, as described by

$$\underbrace{\begin{bmatrix} [Z_{mn}] & [-C_{mn}] \\ [C_{mn}] & [Y_{mn}] \end{bmatrix}}_{[Z']} \begin{bmatrix} J \\ M \end{bmatrix} = \begin{bmatrix} E \\ H \end{bmatrix}, \quad (1)$$

where J and M are the electric and magnetic surface current vectors, E and H are the electric and magnetic field vectors, $[Z_{mn}]$ is the impedance matrix, $[Y_{mn}]$ is the admittance

matrix, matrix $[C_{mn}]$ defines how $[Y_{mn}]$ and $[Z_{mn}]$ are related to one another (linking matrix), and $[Z']$ is the PMCHWT impedance matrix. This specific integral equation formulation was forced into symmetry through the addition of a phase operator multiplied to one of the two equations, which form the basis of the MoM equation set [6], shown by

$$\underbrace{\begin{bmatrix} [Z_{mn}] & -j[-C_{mn}] \\ j[C_{mn}] & [Y_{mn}] \end{bmatrix}}_{[Z]} \begin{bmatrix} J \\ jM \end{bmatrix} = \begin{bmatrix} E \\ jH \end{bmatrix}. \quad (2)$$

In (2), the parameters $[Z_{mn}]$, $[Y_{mn}]$, and $[C_{mn}]$ are the same as those in (1), and $[Z]$ is the symmetric impedance matrix used in the eigenvalue decomposition for obtaining CMs. The phase offset applied to (2) allows the impedance matrix to become symmetric, but the new matrix $[Z]$ no longer meets the criteria for surface equivalent problems to be free of internal resonances. However, the CMs obtained from $[Z]$ are unique as the eigenvalue decomposition solves for all the modes of the object (internal and external resonances). After current normalization is applied to the CMs and the total radiated power of the individual modes is determined, the internal resonances can be removed through post-processing methods including those described in [4] and [6].

The symmetric form of the impedance matrix shown in [6], though accurate, does not detail the problems associated with, or how to force symmetry on, an SIE for an object with different kinds of materials (i.e., conducting, magnetic and dielectric materials). For such a mixed-material object, the original PMCHWT SIE has to be modified [7]. This modification changes the general layout of the original impedance matrix, as is shown by (20) in [7]. This equation can be simplified to be used with any two kinds of materials, in the simplest form a perfect electric conductor (PEC) and a single dielectric material, as shown by

$$\underbrace{\begin{bmatrix} [Z_{m1}] & [C_{m1,1}] & [C_{m1,2}] \\ [-C_{m1,1}] & [Z_{m2}] & [C_{m2}] \\ [-C_{m1,2}] & [-C_{m2}] & [Y_{m2}] \end{bmatrix}}_{[Z']} \begin{bmatrix} J_{m1} \\ J_{m2} \\ M_{m2} \end{bmatrix} = \begin{bmatrix} E_{m1} \\ E_{m2} \\ H_{m2} \end{bmatrix} \quad (3)$$

where $[Z_{m1}]$ is the impedance matrix of material 1, $[Z_{m2}]$ is the impedance matrix of material 2, $[Y_{m2}]$ is the admittance matrix of material 2, and $[C_{m1,1}]$, $[C_{m1,2}]$, $[C_{m2}]$ define how the impedance and admittance matrices ($[Z_{m1}]$, $[Z_{m2}]$, $[Y_{m2}]$) are linked to one another. J_{m1} and E_{m1} are the electric current and electric field vectors of material 1, J_{m2} and E_{m2} are the electric current and electric field vectors of material 2, and M_{m2} and H_{m2} are the magnetic current and magnetic field vectors of material 2. In general, the individual matrices are of different sizes and hence the linking matrices are not guaranteed to be square. Moreover, it can be seen from (3) that $[Z']$ is not symmetric. Therefore, (1) and (3) have the same general form.

The outlined asymmetry problem with mixed-material analysis requires the equation system (3) to be forced into symmetry in the same manner as (1). The resulting symmetric matrix $[Z]$, can be formed as

$$\underbrace{\begin{bmatrix} [Z_{m1}] & -j[C_{m1,1}] & -j[C_{m1,2}] \\ j[-C_{m1,1}] & [Z_{m2}] & -j[C_{m2}] \\ j[-C_{m1,2}] & j[-C_{m2}] & [Y_{m2}] \end{bmatrix}}_{[Z]} \begin{bmatrix} J_{m1} \\ J_{m2} \\ jM_{m2} \end{bmatrix} = \begin{bmatrix} E_{m1} \\ E_{m2} \\ jH_{m2} \end{bmatrix}. \quad (4)$$

When a properly weighted eigenvalue decomposition of the symmetric $[Z]$ as described by (4) is applied, proper diagonalization of the characteristic currents is accomplished. This analysis provides an orthogonal set of currents for the PEC object (material 1) and the associated electric and magnetic surface currents of material 2. However, this formulation is based on the original PMCHWT MoM SIE, and when forced into symmetry, the full set of orthogonal currents will pertain to both non-real CMs (internal resonances) and real CMs. The non-real CMs can be removed through the post-processing methods described in [4] and [6].

III. INTERNAL RESONANCES OF PLANAR STRUCTURES

Internal resonances resulting from the symmetric form of the PMCHWT mixed-material SIE given by (4) can have a significant impact on the CM analysis of a structure which utilizes any amount of dielectrics, planar structures included. The internal resonance problem cannot be predicted, and as such should not be ignored. To illustrate the impact of the internal resonance problem, two different planar structures with the dimensions of 136 mm \times 66 mm were analyzed. These structures are intended to represent the rectangular chassis used in a typical mobile terminal. The first structure was a baseline structure (a flat rectangular plate of zero thickness) utilizing only PEC, as shown in Fig. 1. The CMs of this structure were obtained using the conventional TCM formulation [1]. The second structure, as shown in Fig. 2, was a printed circuit board (PCB). The PCB consisted of the rectangular PEC plate of the first structure as well as a 1 mm FR4 substrate attached to one side of the PEC plate. The substrate provides mechanical support to the terminal chassis and facilitates electronic component integration.

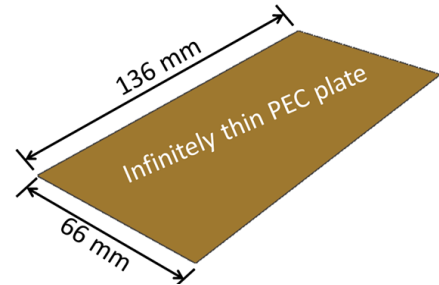


Fig. 1: Flat perfect electric conductor terminal chassis of the first structure.

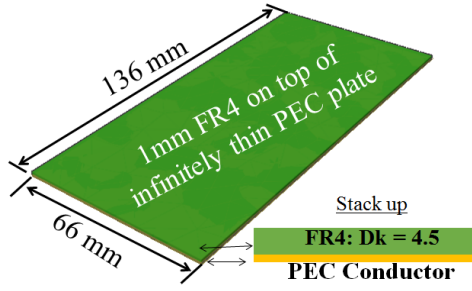


Fig. 2: PEC layer and dielectric substrate forming the chassis of the second structure.

Solving for the CMs of the first structure using standard TCM provides a baseline of the modes that exist in a flat PEC structure (see Fig. 3). However, all commercial terminal chassis utilize PCBs with dielectric substrates. Therefore, the second terminal chassis structure as shown in Fig. 2 better resembles a real-world design. Since this structure contains dielectric material, the CM analysis must be carried out using a symmetric impedance matrix formed by either a VIE or the previously described SIE MoM solution. Solving for the CMs of this structure using a VIE implementation requires a dense tetrahedral mesh which requires significantly more computational time than an SIE implementation. As a rough comparison, the computational time to solve for the CMs (per frequency point) was found to be 226 seconds for a coarse VIE mesh, whereas the computational efficient SIE implementation required only 8.6 seconds (per frequency point). As was illustrated in [6], the computational requirements for a CM VIE implementation is not practical for most engineering applications; hence, the PMCHWT mixed-material SIE formulation (4) is used in this work.

The CM eigenvalues of the second structure are shown as black dots in Fig. 4. In this plot the internal resonances have not yet been removed using post-processing methods. It can be seen from this figure that the calculated modes are significantly different from the modes of the PEC chassis (Fig. 3). Though not likely, these modes could be real CMs as the structure has changed, and thus the two sets of CMs should not be identical. However, the sheer number of CMs present are an indication that internal resonant modes may be found in this solution. When the internal resonances are removed using the post-processing method proposed in [6], the eigenvalues shown by red circles in Fig. 4 remained. It can be observed from this figure that the number of modes matches the number of modes seen in the baseline structure (see Fig. 3). However, minor differences have been found, including a decrease in the resonance frequency for most modes (e.g., from 983 MHz in Fig. 3 to 957 MHz in Fig. 4 for the first real CM), as well as slight differences in each of the modes' quality factor (Q) and current distributions. This is expected, as the dielectric material should load the structure, with some modes being more affected than others.

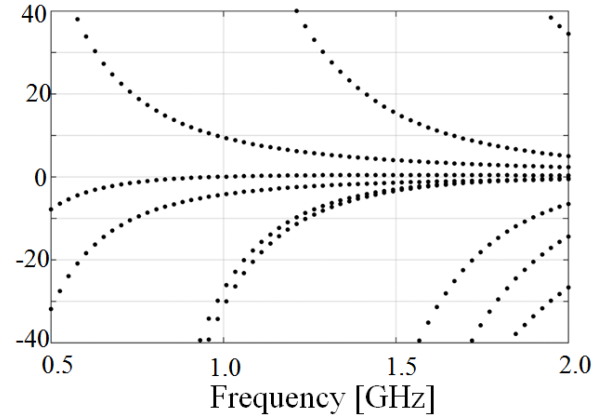


Fig. 3: CMs of the first structure (Fig. 1) as calculated from conventional TCM.

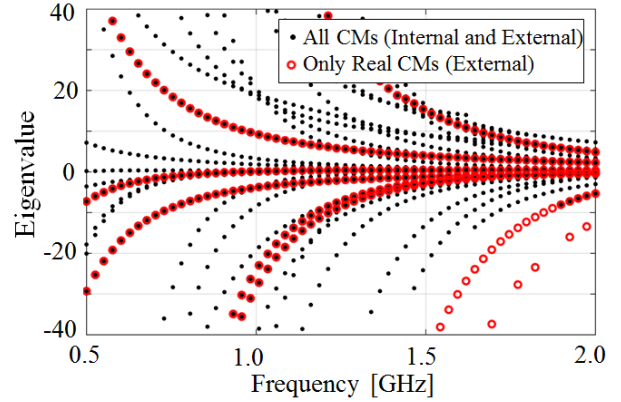


Fig. 4: First 60 modes from SIE formulation (black dots), and all real CMs (red) of the second structure (Fig. 2).

IV. EVALUATION AND EXCITATION ANALYSIS OF CMs

It is possible to use the standard TCM to individually excite specific CMs. Utilizing the attributes associated with the real CMs of the structure, feed placement analysis can be performed on these structures [8]. The first CM of the PEC structure becomes resonant at 983 MHz (see Fig. 3), and the currents of this resonant mode resembles those of a flat dipole along the length of the chassis. These currents could be fed by splitting the chassis in half and feeding the mode using a current based feed (e.g., as is done with a traditional dipole antenna), but this is not practical in most terminal antenna applications. As a traditional current feed should not be applied, analysis of the near-field of this mode must be examined. The near-fields of mode 1 of the PEC structure are shown in Fig. 5. This figure shows that at each end of the chassis there is significant electric near-field energy in the x -direction (along the length of the chassis). Through implementing a capacitive coupling element (CE) located at the end of the chassis (as seen in Fig. 5) the mode can be excited. The second mode of the PEC chassis is resonant at 1.86 GHz. For the same reasons as were described for mode 1, a current based feed is not an appropriate excitation method

for mode 2 and a near-field CE must be utilized. The electric near-fields of mode 2 for the PEC chassis are visualized in Fig. 6. Using this information, it can be determined that a CE located at the edge of the chassis (along the width of the chassis) which couples y -directed energy into the chassis, should excite the mode. The placement and length of this coupling element is shown in Fig. 6.

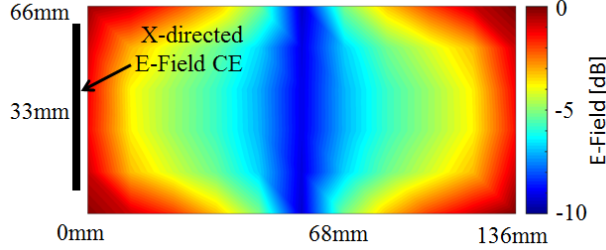


Fig. 5: Mode 1 of PEC chassis and mode 2 of the mixed-material chassis.

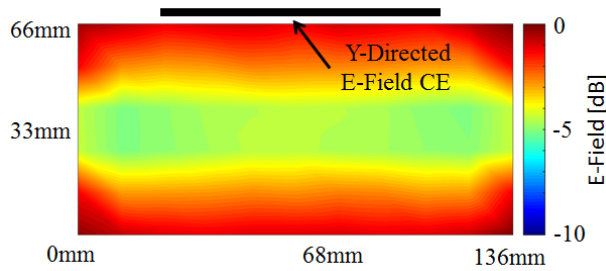


Fig. 6: Mode 2 of the PEC chassis and mode 5 of the mixed-material chassis.

The total number of CMs in the mixed-material chassis far exceeds the number of modes calculated for the PEC chassis. Both [4] and [6] indicate that many of these modes should not be considered real CMs. Furthermore, those modes indicated to be non-real CM should not be excitable. To determine if these modes are excitable the first and second CM of the mixed material chassis can be examined. The first CM is considered (by means of post-processing) to be a non-real CM, whereas the second CM is a real CM. The first CM of this structure becomes resonant at 462 MHz, and this mode has a seemingly random current distribution with no apparent locations where the chassis can be segmented and fed using a current feed. The less random electric near-field distribution has two locations where a CE could be utilized to excite the structure (points 'A' and 'B' in Fig. 7). Although excitation of the structure may be achievable using these CE locations, successful feed excitation does not imply that mode 1 is excited, but rather another mode may be excited. This is because it is physically possible to use an impedance matching network to force a non-resonant mode into resonance. Mode 2 of the structure has a nearly identical current distribution as that of mode 1 in the PEC chassis. This mode is resonant at 957 MHz, and can be excited with the same CE which was used to excite mode 1 of the PEC chassis (Fig. 5). Furthermore, mode 6 of the mixed-material chassis closely resembles the current distribution and resonant

frequency of mode 2 of the PEC chassis (Fig. 6).

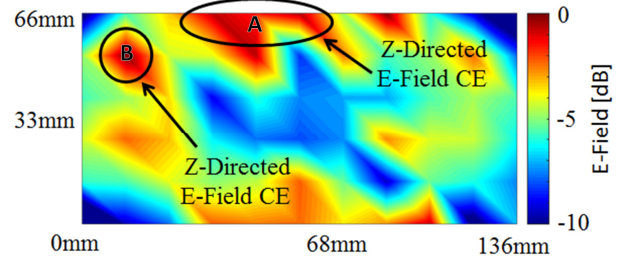


Fig. 7: Mode 1 of the mixed-material chassis.

The CE feed elements can be implemented in a full-wave simulation program and the feed-excited CMs of each chassis can be reconstructed using the theory presented in [9]. This theory allows the far-fields of the structure to be compared against the characteristic far-fields. If the excited chassis does not match that of the intended CM, the mode was not excited and the mode can be attributed to a non-real CM.

V. VERIFICATION OF MODES

The different antenna structures described in Section IV were simulated in the FEM solver of CST. Mode 1 of the PEC chassis (Mode 2 of the mixed-material chassis) was fed using a $50 \text{ mm} \times 4 \text{ mm}$ CE located 2 mm from the chassis and a capacitive lumped element was used to achieve the resonant frequency of 981 MHz (944 MHz). Mode 2 of the PEC chassis (mode 6 of the mixed-material chassis) was fed using a $100 \text{ mm} \times 4 \text{ mm}$ CE at 2 mm from the edge, a two element L matching network allowed for the resonant frequency of 1.82 GHz to be realized. Five simulations were carried out in an effort to excite Mode 1 of the mixed-material chassis. The first set of simulations utilized a $26 \text{ mm} \times 2 \text{ mm}$ plate, placed at 3 mm, 5 mm, and 7 mm above the chassis (indicated by modes 1a, 1b, and 1c in Table I) at the feed location indicated by point 'A' in Fig. 7. The second set of simulations utilized a $10 \text{ mm} \times 10 \text{ mm}$ CE placed at 4 mm and 6 mm above the chassis (indicated by modes 1d and 1e in Table I) at the feed location shown by point 'B' in Fig. 7. In these simulations an ideal π matching network was utilized in an effort to achieve a resonant frequency near 462 MHz. It should be noted that the far-fields of mode 1 of the mixed-material chassis is highly correlated with that of mode 2 (42% in envelope correlation), whereas those of modes 2 and 6 are fully uncorrelated (as were modes 1 and 2 of the PEC chassis). The bandwidth of modes 1a-1e were found to be less than 0.4% while all other modes had a resonant bandwidth of greater than 6%. The far-fields obtained from the CM analysis, and the FEM analysis, were applied to the theory presented in [9], and the results are shown in Table I. This table shows that the PEC structure was excited and the modes of interest were reconstructed to a high degree. The presence of mode 1 in the mixed-material chassis changed significantly between the two different feed positions, and mode 1 maintained a relatively low effective bandwidth across all feed types and locations. This behavior confirms mode 1

being a non-real CM. The relative Q of mode 1 is nearly equivalent to that of mode 2, but the latter achieved a bandwidth of 6.2%. Furthermore, the FEM excitation of mode 2 was fully reconstructed to the intended CM in the mixed material chassis, relating this mode to a real external resonant mode. It is also noted that, due to the correlation between modes 1 and 2 in the mixed-material structure, the sum of the percentages of contributing modes for each of these mixed-material cases exceeds 100%.

TABLE I. MODAL RECONSTRUCTION FOR PEC AND MIXED-MATERIAL TERMINAL CHASSIS

Structure	Mode	Reconstruction		
		Mode 1	Mode 2	Mode 6
PEC	Mode 1	94%	2%	0%
PEC	Mode 2	1%	96%	0%
Mixed	Mode 1a	16%	46%	52%
Mixed	Mode 1b	14%	48%	56%
Mixed	Mode 1c	17%	44%	58%
Mixed	Mode 1d	29%	90%	4%
Mixed	Mode 1e	36%	88%	4%
Mixed	Mode 2	40%	98%	0%

VI. CONCLUSION

The CMs of a structure are dependent on the materials used to form the structure. Dielectric and magnetic materials load resonant structures differently and dielectric objects have the ability to become self-resonant. To determine the influence of mixed-material objects on the inherent CMs, symmetry must be forced on the SIE utilized to solve the problem. The symmetric PMCHWT mixed-material SIE impedance matrix is

not free of the internal resonance problem, and as such non-real CMs are found in the CM solution set. When the CMs of a mixed-material object are analyzed the modes attributed to non-real CMs (internal resonances), as determined by post-processing, cannot be excited or reconstructed using full-wave analysis. These non-excitable modes are thus considered to be non-real CMs and should be removed before traditional CM analysis is applied.

REFERENCES

- [1] R. F. Harrington and J. R. Mautz, "Theory of characteristic modes for conducting bodies," *IEEE Trans. Antennas Propag.*, vol. 19, no. 5, pp. 622-628, Sep. 1971.
- [2] R. F. Harrington, J. R. Mautz, and Y. Chang, "Characteristic modes for dielectric and magnetic bodies," *IEEE Trans. Antennas Propag.*, vol. 20, no. 2, pp. 194-198, Mar. 1972.
- [3] W. C. Chew, M. S. Tong, and B. Hu, "Integral equations for electromagnetic and elastic waves," in *Lectures on Computational Electromagnetics #12*, 1st ed. San Rafael, CA., USA: Morgan Claypool, 2009, ch. 3-4, pp. 43-102.
- [4] H. Alroughani, J. L. T. Ethier, and D. A. McNamara, "Observations on computational outcomes for the characteristic modes of dielectric objects," in *Proc. Int. Symp. Antennas Propag.*, Memphis, TN, USA, Jul. 6-11, 2014, pp. 844-845.
- [5] Y. Chang and R. F. Harrington, "A surface formulation for characteristic modes of material bodies," *IEEE Trans. Antennas Propag.*, vol. 25, no. 6, pp. 789-795, Nov. 1977.
- [6] Z. Miers and B. K. Lau, "Computational analysis and verifications of characteristic modes in real materials," *IEEE Trans. Antennas Propag.*, in major revision.
- [7] A. A. Kishk and L. Shafai, "Different formulations for numerical solution of single or multibodies of revolution with mixed boundary conditions," *IEEE Trans. Antennas Propag.*, vol. 34, no. 5, pp. 666-673, May 1986.
- [8] Z. Miers, H. Li, and B. K. Lau, "Design of bandwidth-enhanced and multiband MIMO antennas using characteristic modes," *IEEE Antennas Wireless Propag. Lett.*, vol. 12, pp. 1696-1699, 2013.
- [9] E. Safin and D. Manteuffel, "Reconstruction of the characteristic modes on an antenna based on the radiated far field," *IEEE Trans. Antennas Propag.*, vol. 61, no. 6, pp. 2964-2971, Jun. 2013.